

See discussions, stats, and author profiles for this publication at: <https://www.researchgate.net/publication/233799560>

# Rheology of Polypropylene/Clay Hybrid Materials

ARTICLE *in* MACROMOLECULES · MARCH 2001

Impact Factor: 5.8 · DOI: 10.1021/ma001122e

---

CITATIONS

467

---

READS

149

5 AUTHORS, INCLUDING:



**Abdulwahab Almusallam**

Kuwait University

25 PUBLICATIONS 777 CITATIONS

SEE PROFILE



**Anongnat Somwangthanaroj**

Chulalongkorn University

22 PUBLICATIONS 758 CITATIONS

SEE PROFILE



**Priya Varadan**

University of Michigan

5 PUBLICATIONS 689 CITATIONS

SEE PROFILE

## Rheology of Polypropylene/Clay Hybrid Materials

Michael J. Solomon,<sup>\*,†,‡</sup> Abdulwahab S. Almusallam,<sup>†</sup> Kurt F. Seefeldt,<sup>†</sup>  
Anongnat Somwangthanaroj,<sup>‡</sup> and Priya Varadan<sup>†</sup>

Department of Chemical Engineering and Macromolecular Science and Engineering Program,  
University of Michigan, Ann Arbor, Michigan 48109

Received June 27, 2000; Revised Manuscript Received December 5, 2000

**ABSTRACT:** The melt-state linear and nonlinear shear rheological properties of hybrid materials of polypropylene and amine-exchanged montmorillonite were studied. The materials were prepared by melt mixing with maleic anhydride functionalized polypropylene as the compatibilizer. The clay interlayer spacing (as determined by wide-angle X-ray scattering) increased upon melt mixing; however, the short-range ordering of the clay layers was preserved. Above inorganic loadings of 2.0 wt % the hybrid materials exhibited apparent low-frequency plateaus in the linear viscoelastic moduli. The hybrid storage modulus was sensitive to the chemistry of the amine exchanged into the clay. The amount of stress overshoot observed in flow reversal experiments was found to be a function of the rest time allowed between the reversal. The transient stress in start-up of steady shear scaled with the applied strain. These observations allow features of the polypropylene/montmorillonite hybrid structure to be deduced. The transient nonlinear rheology is consistent with an anisometric, non-Brownian structure. These anisometric particulate domains are mesoscopic, and internally, they contain multiple, ordered platelets. This mesoscopic structure is itself thermodynamically unstable, because the rheology indicates that quiescent structural evolution whose origin is not Brownian relaxation is observed. The demonstration of the sensitivity of melt-state rheological measurements to interparticle structure and chemistry of the hybrid materials indicates the potential usefulness of such studies for the development of new nanocomposite materials.

## I. Introduction

The blending of polymers with inorganic particles has long been recognized as an economical method to produce new materials. Recently, mixtures of polymers and layered smectite clays have been prepared with significantly enhanced solid-state mechanical, dimensional, permeability, and flame-retardant properties relative to the pure polymer. These enhancements have been achieved at low clay particle loadings, typically in the range 1–10 wt %. For example, mixtures of nylon-6 and the smectite clay montmorillonite exhibit heat distortion temperatures that are more than 90 °C greater than pure nylon at less than 5 wt % clay loading.<sup>1</sup> The tensile modulus of epoxy/clay hybrids at 10 wt % concentration is a factor of 6 greater than the neat epoxy.<sup>2</sup> Improvements in the barrier properties of poly( $\epsilon$ -caprolactone) nanocomposites and the fire resistance of nylon-6/clay hybrids have also been reported.<sup>3,4</sup> It is projected that polymer/clay hybrids, so-called nanocomposites, will find use as new materials in automotive, packaging, and aerospace applications.<sup>5</sup>

In its natural form, smectite clay such as Na–montmorillonite has a layered structure. The interlayer dimension is determined by the crystal structure of the aluminosilicate. For dehydrated Na–montmorillonite, this dimension is approximately 1.0 nm. The lateral dimensions of the discotic clay particles are determined by the method of preparation. Clays prepared by milling typically have lateral platelet dimensions of approximately 0.1–1.0  $\mu$ m. Because of its colloidal size and large aspect ratio, delaminated clay possesses an extremely large surface area. It has been hypothesized that large surface area, high aspect ratio, and good

interfacial interaction are essential to produce enhanced solid-state properties in composite materials.<sup>6</sup> Thus, the optimal nanocomposite structure is thought to consist of disordered, exfoliated clay platelets dispersed in a polymer matrix.

The development of the desired clay morphology has been accomplished by two methods: in-situ polymerization and melt mixing. The first step in both methods involves the preparation of organophilic clay. Natural clay is hydrophilic, and the polymer in which it is to be dispersed is often hydrophobic. Thus, surfactants, typically aliphatic amines, are introduced in the gallery regions between the clay layers by means of cation exchange. This process renders the clay more hydrophobic. The intercalated amine species thereby improve compatibility with the polymeric host while also increasing the clay layer interlayer spacing.<sup>7</sup> Then, in preparation by in-situ polymerization, a polymer precursor is infiltrated into the intercalated, organophilic clay. Polymerization produces long-chain polymers within the clay galleries. Under conditions in which intra and extra gallery polymerization rates are properly balanced, the clay layers are delaminated, and the resulting material possesses a disordered structure. Alternatively, in preparation by melt mixing, the organophilic clay is melt mixed with the polymeric host and, possibly, compatibilizing additives.<sup>8</sup> Increased intercalation and exfoliation result if the organophilic clay possesses sufficient affinity for the host and additive. Nylon, polystyrene, polypropylene, and poly(ethylene oxide) clay hybrids have all been prepared by melt mixing.<sup>9–13</sup>

It is instructive to study the rheology of polymer/clay hybrids for two reasons. First, rheological properties are indicative of melt-processing behavior in unit operations such as injection molding. Second, since the rheological properties of particulate suspensions are sensitive to the

<sup>†</sup> Department of Chemical Engineering.

<sup>‡</sup> Macromolecular Science and Engineering Program.

structure, particle size, shape, and surface characteristics of the dispersed phase, rheology potentially offers a means to assess the state of dispersion of nanocomposites directly in the melt state. Thus, rheology can be envisaged as a tool that is complementary to traditional methods of materials characterization such as electron microscopy, X-ray scattering, dynamic mechanical analysis, and mechanical testing. The advantages of rheology relative to these methods are that measurements are performed in the melt state and that a battery of different rheological methods can be used to study the response of the nanocomposite structure to both linear and nonlinear deformation. A disadvantage of rheological methods is that they probe the hybrid structure only indirectly. Previous rheological studies of nanocomposites have focused on oscillatory and steady-shear studies of nylon and polystyrene/polyisoprene block copolymer materials.<sup>14–16</sup>

This study explores the linear and nonlinear rheology of polypropylene/montmorillonite hybrid materials. The particular combination of polymer and clay was chosen because of its potential commercial relevance as an automotive material and because of recent literature reports of its successful preparation.<sup>10,11,17–19</sup> Materials were prepared according to the method of Kawasumi et al.<sup>11</sup> Na–montmorillonite clay was rendered organophilic by cation exchange with a long chain amine, such as stearylamine. It was then melt mixed with polypropylene and a maleic anhydride functionalized polypropylene additive. Materials with inorganic particle loading in the range 1.3–6.2% (inorganic weight basis) were prepared. Solid-state material properties were characterized by means of wide-angle X-ray scattering and dynamic mechanical analysis. Measurements of linear viscoelasticity revealed the effect of adding clay to the polypropylene host. Start-up of steady shear and flow reversal studies probed the nonlinear rheological properties of the polypropylene nanocomposites. The effect of particle loading on each of the rheological measures was studied. The effects of the chemistry of the exchanged amine on the linear viscoelastic moduli were probed. The results are interpreted in light of recent rheological studies of nylon and polystyrene/polyisoprene nanocomposites.<sup>14–16</sup> The thermodynamic behavior and phase stability of the hybrid materials, which have been recently studied by means of self-consistent-field theory and density functional theory, respectively,<sup>20,21</sup> are also discussed. Particular emphasis is placed on deducing the interparticle structure of the hybrid materials from the linear and nonlinear rheological measurements. The characteristic dimension of structure in the hybrids is the focus of analysis because large inorganic structures are thought to be less optimal for the development of the valuable end-use properties of polymer nanocomposites.

## II. Materials and Methods

**Materials and Preparation.** Polymer/clay hybrid materials were prepared by melt mixing of organophilic clay, polypropylene, and compatibilizer. The clay was a high-purity Na–montmorillonite prepared from natural bentonite (Mineral Colloid BP, Southern Clay products, Gonzales, TX, cation exchange capacity (CEC) =  $90 \pm 1$  mequiv/100 g). Organophilic clay was prepared by cation exchange of natural counterions with amine surfactants according to the method of Kawasumi et al.<sup>11</sup> The amines used were stearylamine (C-18 amine, Aldrich), tridecylamine (C-13 amine, Aldrich), and di-tridecylamine (2C-13 amine, BASF). The 2C-13 amine was solubilized

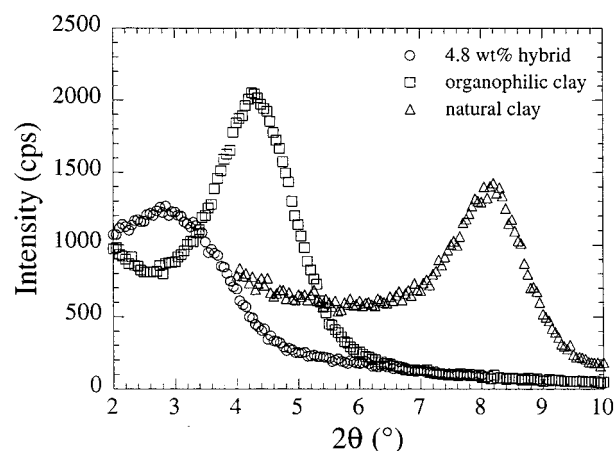


**Figure 1.** Comparison of ambient temperature wide-angle X-ray scattering of the natural clay, C-18 amine exchanged clay, and a polypropylene hybrid material with 4.80 wt % inorganic content prepared by melt mixing. Here, and for all subsequent figures, the compatibilizer is maleic functionalized polypropylene ( $M_w = 92\,000$  g/mol, MA content = 0.43 wt %). The ratio of organophilic clay to compatibilizer is 1:3 on a weight basis.

**Table 1. Clay Interlayer Spacing from Figure 1**

|                        | natural<br>clay | C-18 amine<br>exchanged clay | 4.80 wt %<br>hybrid material |
|------------------------|-----------------|------------------------------|------------------------------|
| interlayer spacing (Å) | 11              | 21                           | 29                           |

in ethanol at 60 °C before use in the cation exchange reaction. The clays were freeze-dried after precipitation and rinsing.

The organophilic clay was blended with polypropylene (Equistar Chemicals,  $M_w = 246\,200$  g/mol and  $M_w/M_n = 6.1$  from gel permeation chromatography) and the compatibilizer maleic anhydride functionalized polypropylene (Uniroyal Chemical,  $M_w = 92\,000$  g/mol,  $M_w/M_n = 2.6$  from gel permeation chromatography, maleic anhydride (MA) content 0.43 wt %). The anhydride content was determined by the method described in Sclavons et al.<sup>22</sup> The inorganic content of the blends varied from 1.30 to 6.17 wt %. The weight ratio of organophilic clay to compatibilizer was 1:3 in all cases. Melt mixing was performed in a nitrogen environment in a Banbury mixer attached to a Braebender plasticorder. Materials were mixed at a temperature of 175 °C (measured by internal thermocouple) for 40 min after melting of the polymeric constituents. Approximately 38 g of polymer/clay hybrid was prepared per batch.

**X-ray Diffraction.** Wide-angle X-ray scattering (WAXS) was conducted at ambient temperature on a Rigaku rotating anode diffractometer with Cu K $\alpha$  radiation of wavelength 1.54 Å. The accelerating voltage was 40 kV. Natural montmorillonite and the freeze-dried organophilic clay were studied as powders. The blended materials were prepared in films of 400  $\mu$ m thickness by compression molding.

Results of WAXS are plotted in Figure 1. The angular dependence of the scattering intensity is reported for a hybrid material with 4.80 wt % inorganic content, for the stearylamine exchanged clay powder, and for the natural clay powder. The peaks correspond to the {001} basal reflection of the montmorillonite aluminosilicate. From the angular location of the peaks and the Bragg condition the interlayer spacing of each of the samples was determined. The computed values are reported in Table 1. The difference in the interlayer spacing between the natural and organophilic clay is due to the intercalation of stearylamine. The slightly increased interlayer spacing after melt mixing is presumably due to additional intercalation of polymeric species. Note that the existence of Bragg peaks in the melt mixed materials shows that the nanocomposite still retains an ordered structure after melt mixing. The WAXS results are in qualitative agreement with results for other polypropylene hybrids<sup>10,11</sup> and thereby

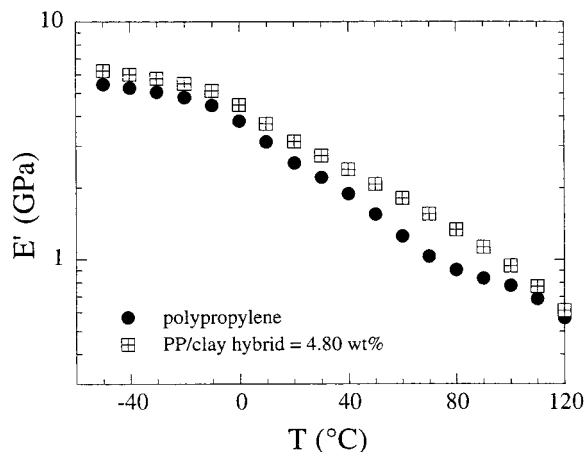


**Figure 2.** Temperature dependence of the tensile modulus of pure polypropylene and the 4.80 wt % hybrid material as determined by dynamic mechanical analysis at an oscillatory frequency of 10 Hz.

**Table 2.** WAXS-Derived Interlayer Spacing for Hybrid Materials of Figure 8

| interlayer spacing (Å) | organophilic montmorillonite powder | 4.8 wt % clay hybrid material |
|------------------------|-------------------------------------|-------------------------------|
| C-13 amine             | 19                                  | 22                            |
| C-18 amine             | 21                                  | 29                            |
| 50/50 C-18/2C-13 amine | 26                                  | 28                            |
| 2C-13 amine            | 25                                  | 25                            |

serve as a confirmation of our method of preparation. X-ray diffraction studies were conducted for all hybrids prepared. The location of the peaks showed no batch to batch variation or significant dependence on the inorganic content of the hybrid. The WAXS-derived interlayer spacing of other materials used in the rheological studies is reported in Table 2.

**Dynamic Mechanical Analysis.** Dynamic mechanical analysis was performed in tensile mode between  $-50$  and  $120$  °C at a frequency of 10 Hz (TA Instruments dynamic mechanical analyzer, DMA 2980). Test samples were prepared by compression molding. The temperature dependence of the tensile storage modulus ( $E'$ ) of a 4.80 wt % polypropylene/montmorillonite hybrid and of polypropylene is plotted in Figure 2. The increase in modulus due to the clay is modest; however, the difference between the two becomes significant for  $40$  °C  $< T$  (°C)  $< 100$  °C, approximately. The maximum modulus enhancement is approximately 40% at  $T \sim 70$  °C. The amount of modulus enhancement agrees with the results Kawasumi et al.<sup>11</sup>

**Rheology.** Small-amplitude oscillatory shear, start-up of steady shear, and flow reversal studies were conducted on a controlled strain rate rheometer (ARES rheometer, Rheometrics Scientific, NJ) in a nitrogen environment. Most studies were performed at 180 °C, although linear viscoelastic measurements were conducted over the range 165–210 °C to allow time–temperature superposition. Test specimens were prepared by compression molding.

The region of linear viscoelastic behavior was very sensitive to the presence of clay. Figure 3 plots the strain dependence of the normalized (nonlinear) storage modulus for a 4.80 wt % hybrid and pure polypropylene. The deviation from linear behavior for the hybrid materials occurs at a strain that is approximately 2 orders of magnitude less than for pure polypropylene. The small-amplitude studies of oscillatory shear of the hybrid materials where conducted in the interval  $0.005 < \gamma_0 < 0.01$ .

Because of the potential for solidlike or slowly relaxing fluid structure in the hybrid materials, the prior deformation history of the samples was carefully controlled. For the linear viscoelastic measurements and start-up of steady shear measurements, samples were equilibrated in the rheometer after

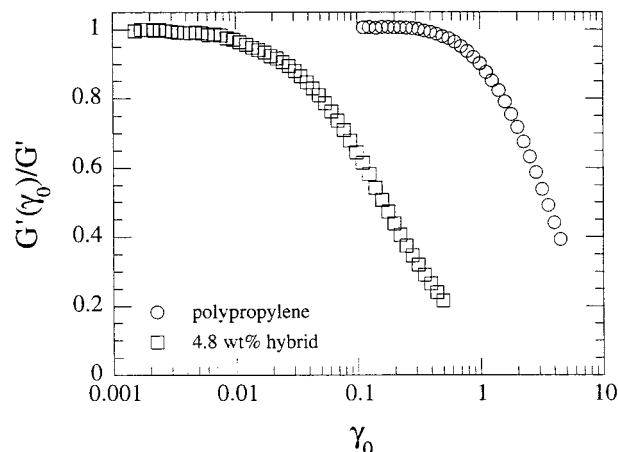


**Figure 3.** Strain dependence of the in-phase component of the stress response to oscillatory shear for polypropylene and the 4.80 wt % hybrid material at  $T = 180$  °C and  $\omega = 1.0$  s $^{-1}$ .

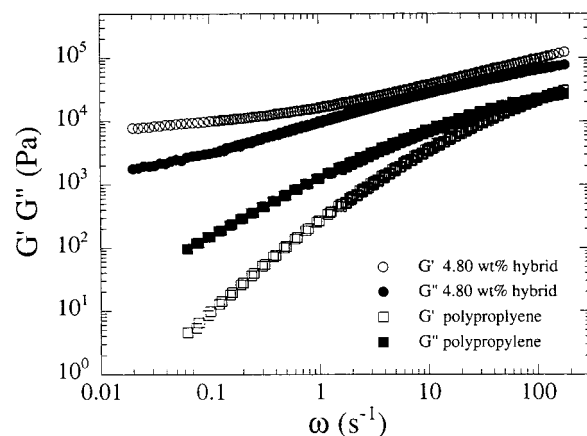


**Figure 4.** Comparison of the storage ( $G'$ ) and loss ( $G''$ ) modulus of the 4.80 wt % hybrid material and pure polypropylene. The master curves, obtained by time–temperature superposition, are plotted at the reference temperature  $T = 180$  °C.

loading at the desired temperature for one-half hour prior to testing. During this period, the storage modulus was monitored. No significant changes were observed beyond one-half hour, thereby indicating that a reproducible initial state had been achieved. Note that initial state for the flow reversal experiments was established differently, as described in the next section.

### III. Results

**Linear Viscoelasticity.** Master curves of the storage and loss moduli ( $G'$ ,  $G''$ ) of a 4.8 wt % polypropylene montmorillonite hybrid and pure polypropylene are compared in Figure 4. The intercalating species was C-18 amine, and the compatibilizer was maleic anhydride functionalized polypropylene (PP-MA) with  $M_w = 92\,000$  g/mol. Measurements were performed over the temperature range 165–210 °C, and time–temperature superposition was performed relative to 180 °C. Comparison of the linear viscoelastic response of the two materials shows the significant effect of the clay, particularly at low frequencies. The apparent plateau in  $G'$  and  $G''$  at low frequencies for the hybrid material is consistent with either the response of a viscoelastic solid or a viscoelastic fluid with a characteristic relaxation time that is much larger than  $10^2$  s, since no terminal regime is observable for  $\omega > 0.01$  s $^{-1}$ . As



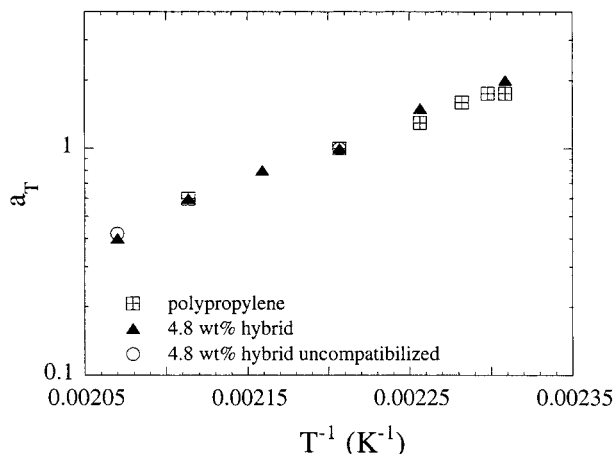


**Figure 5.** Temperature dependence of the shift factors for polypropylene, the 4.80 wt % compatibilized hybrid material, and the 4.80 wt % uncompatibilized hybrid material as derived by means of time–temperature superposition. The clay has been C-18 amine exchanged.

considered in the discussion, the observed linear viscoelasticity could be explained by the existence of a percolated, network microstructure or by the rotational relaxation of anisometric clay platelets or platelet domains.

The horizontal shift factors,  $a_T$ , used to construct Figure 4 are plotted in Figure 5. (Note that no vertical shifts to the data were required to achieve time–temperature superposition.) To within experimental error, the shift factors of pure polypropylene and the compatibilized hybrid are identical. The shift factors for an uncompatibilized hybrid material at the same inorganic particle loading are also plotted for comparison. The observation that the addition of inorganic clay significantly affects the magnitude of  $G'$  and  $G''$  but not the characteristics of the time–temperature superposition has previously been observed for nylon and polystyrene/polyisoprene block copolymer nanocomposites.<sup>15,16</sup> As considered in section IV and recognized by Ren et al., this peculiar time–temperature superposition behavior is linked to the non-Brownian structure of the hybrid materials.

To further aid in distinguishing among the hypothetical microstructures, the effect of particle loading on the polypropylene/montmorillonite hybrid linear viscoelasticity was investigated. The inorganic concentration of clay was varied from 1.30 to 6.17 wt %. Results for the dependence of the storage modulus on clay loading are plotted in Figure 6. Not shown are results that indicate analogous trends for the loss modulus. In Figure 6,  $G'$  exhibits a complex dependence on the concentration of clay. At the highest frequencies probed,  $G'$  monotonically increases with particle loading; however, low-frequency data for the intermediate concentrations show an inverse dependence on particle loading. Insight into this unusual behavior can be obtained by noting that materials were prepared (after Kawasumi et al.)<sup>11</sup> such that the ratio of organophilic clay to maleic anhydride functionalized compatibilizer was held constant at a 1:3 ratio. Thus, the absolute percentage of maleic anhydride functionalized polypropylene varies from sample to sample in Figure 6. Independent of clay loading effects, the maleic anhydride functionalized polypropylene can itself have two possible effects on melt rheology. First, the lower molecular weight material can plasticize the polypropylene matrix.<sup>23</sup> Second, maleic anhydride may

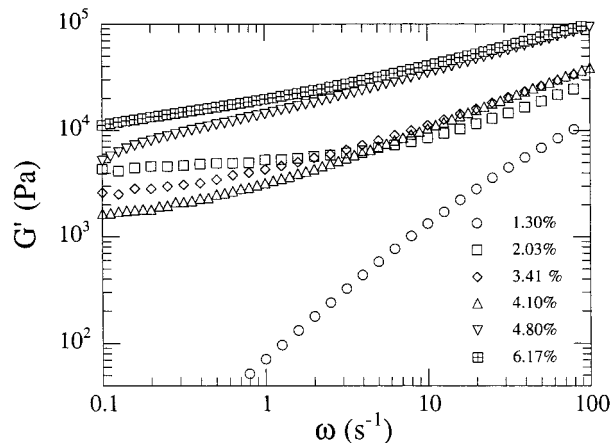


**Figure 6.** Effect of inorganic particle loading on the storage modulus of polypropylene hybrid materials. The measurements were performed at  $T = 180^\circ\text{C}$ . Note that the weight basis ratio of organophilic clay to compatibilizer was held constant at 1:3 for all samples.

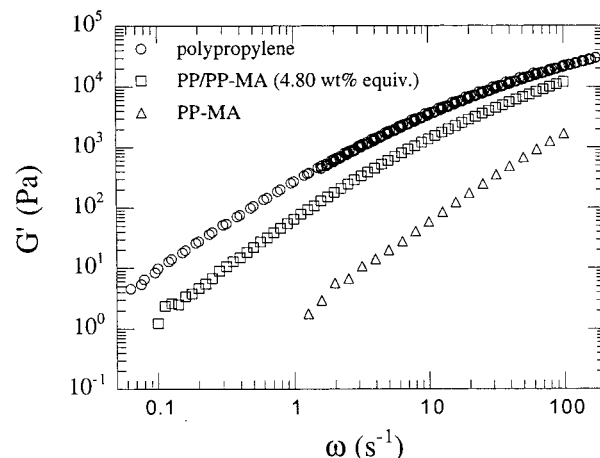


**Figure 7.** Comparison of the linear viscoelastic moduli of pure polypropylene, pure maleic anhydride functionalized polypropylene, and a blend of the two that corresponds to the weight ratios present in the hybrid material with 4.80 wt % inorganic content. Measurements are for  $T = 180^\circ\text{C}$ .

promote chain scission of the neat polypropylene.<sup>24</sup> Both effects would explain the trend in Figure 6 since each would contribute to a reduction in viscosity and elasticity of the matrix in which the clay particles were dispersed, while the clay particles themselves would enhance viscosity and elasticity. The tradeoff between these two competing effects could give rise to a non-monotonic dependence of the storage modulus on particle concentration.

To assess the degree to which such variation could explain the results of Figure 6, the linear viscoelastic properties of polypropylene, the maleic anhydride functionalized polypropylene (PP-MA,  $M_w = 92\,000$  g/mol, MA content = 0.43 wt %), and a blend of the two were measured. The blend, the composition of which corresponded to the amount of compatibilizer present in the 4.8 wt % hybrid material, was prepared by melt mixing under the same conditions as the hybrids. The results, plotted in Figure 7, show that blending the functionalized polypropylene with polypropylene reduces  $G'$  at  $T = 180^\circ\text{C}$  for all frequencies studied. The behavior observed in Figure 7 could provide one contribution to the observed nonmonotonic dependence of  $G'$  on clay loading observed in Figure 6. In fact, a

nonmonotonic effect of maleic anhydride concentration on the storage modulus has even been observed in a series of polypropylenes that were functionalized by melt mixing.<sup>24</sup>

Finally, we note that the trend in Figure 6 could also possibly be explained by real differences in the clay structure of the samples, perhaps caused by an effect of particle loading on the phase behavior of the hybrids or the efficacy of the melt mixing by which they were prepared. In light of the many competing hypotheses, additional experiments are required to understand the effect of particle loading on the structure of the polypropylene hybrid materials.

**Effect of Hybrid Chemistry on Linear Viscoelasticity.** It is reasonable to hypothesize that modifications to the surface characteristics of the clay particles would affect linear viscoelastic properties of the resulting hybrid materials. Such effects might be mediated by changes in mesoscopic clay structure, short-range clay ordering, or surface interactions between the clay and polymer matrix. Thus, probing the effect of hybrid chemistry on rheology potentially yields information regarding such interactions and structure.

The possible effects of the chemistry of the organophilic clay on rheology were investigated by preparation of a series of hybrid materials in which the intercalating surfactant was varied. Briefly, organophilic clays containing stearylamine (C-18 amine), tridecylamine (C-13 amine), ditridecylamine (2C-13 amine), and a 50/50 (mol/mol) mixture of C-18 and 2C-13 amine were prepared by ion exchange. The clays were then melt mixed with polypropylene and the polypropylene compatibilizer (PP-MA,  $M_w = 92\,000$  g/mol, MA content = 0.43 wt %). The results of WAXS studies performed on the resulting clay powders and hybrid materials are included in Table 2. The use of the two-tail surfactant (2C-13 amine) for ion exchange appears to increase the interlayer spacing of the smectite clay powders relative to the results for the single tail surfactants. However, this relative increase is not perpetuated upon melt mixing, since the interlayer spacing of the 2C-13 intercalated clay hybrids is similar to the 2C-13 intercalated clay powders. In fact, Table 2 shows that the hybrid prepared with C-18 intercalated clay was the only material to show a substantial increase in interlayer spacing upon melt mixing.

Although WAXS cannot probe diffraction with inverse wave vector greater than a few nanometers, rheology may well be more sensitive to such mesoscopic structure. Figure 8 shows the effect that organophilic treatment has on the storage modulus of hybrids with 4.8 wt % inorganic content. The sensitivity of hybrid rheology to surfactant chemistry is striking, particularly when compared to the small effect this variable has on the WAXS-derived interlayer spacing. Possible origins of this effect will be discussed in section IV.

**Nonlinear Rheological Properties.** Although the effect of particle loading was probed in the linear viscoelastic regime, concomitant changes to the compatibilizer concentration necessary to maintain the 3:1 compatibilizer-to-clay ratio frustrated efforts to deduce trends from the data. Nonlinear rheological measurements, however, might well be less sensitive to such effects, particularly in cases where flow-induced orientation of the inorganic particle structure dominates the response. For example, as shown in Figure 9, increasing the concentration of clay in the hybrid contributes to a

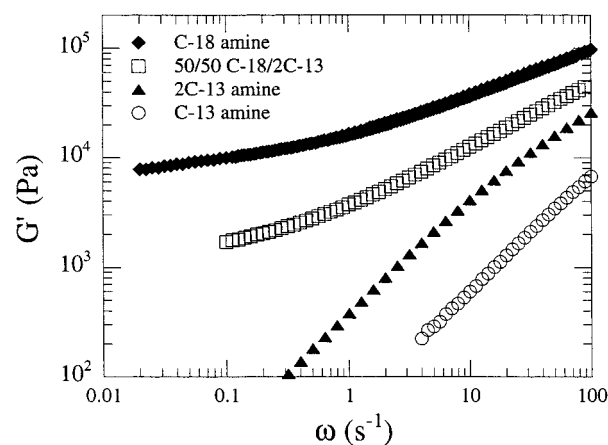


**Figure 8.** Effect of intercalating amine surfactant on the storage modulus of 4.80 wt % compatibilized hybrid materials at  $T = 180$  °C. C-18 amine is stearylamine, 2C-13 amine is ditridecylamine, and C-13 is tridecylamine. 50/50 C-18/2C-13 denotes a 50/50 (weight basis) mixture of the C-18 amine and 2C-13 amine.

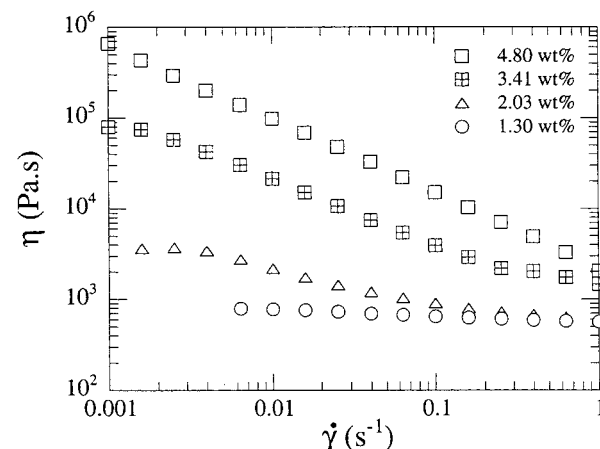


**Figure 9.** Shear rate dependence of the steady-state viscosity of polypropylene hybrid materials of various inorganic content. The measurements were performed at  $T = 180$  °C. The exchanged surfactant is C-18 amine. The compatibilizer is PP-MA ( $M_w = 92\,000$  g/mol, MA content = 0.43 wt %).

large increase in the low-shear rate steady viscosity of the hybrids. In fact, at high particle loadings, no evidence of a low-shear plateau viscosity is exhibited. Significant shear thinning has previously been observed in other kinds of polymer/clay hybrid materials.<sup>14</sup>

Although the shear rate dependence of the steady-shear viscosity suggests that flow modifies the hybrid structure, the transient response to nonlinear deformation is perhaps a more effective test, since structural evolution and relaxation can be quantified. Flow reversal experiments, which have been used to probe such effects in textured solutions of liquid crystalline polymers, are an example of such a test to probe changes in structure.<sup>25</sup> For flow reversal experiments, the following deformation history was applied to the sample: First, the sample was sheared for 300 s at  $\dot{\gamma} = 0.1$  s<sup>-1</sup>. Next, the flow was stopped, and the sample was held quiescently for a time that varied according to the experiment. Finally, the sample was subjected to shear in the reverse direction for 300 s at  $\dot{\gamma} = 0.1$  s<sup>-1</sup>. The shear stress was monitored during this period. Data for the 4.80 wt % hybrid material are plotted in Figure 10. The stress response displays an overshoot, the magnitude of which is a strong function of the amount of time that

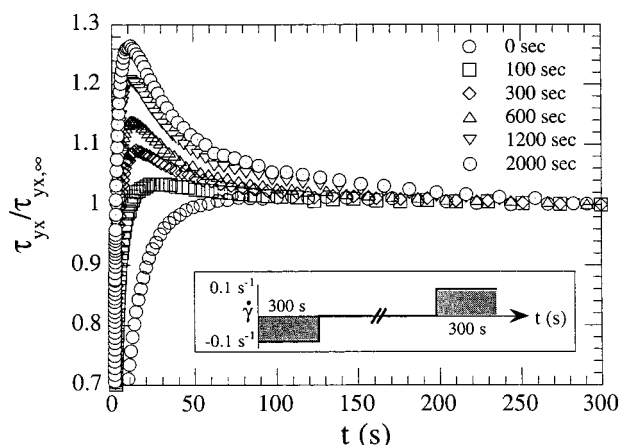


**Figure 10.** Results of flow reversal studies of the 4.80 wt % hybrid material (surfactant: C-18 amine; compatibilizer: PP-MA) at  $T = 180\text{ }^{\circ}\text{C}$ . After an initial episode of steady shear ( $\dot{\gamma} = 0.1\text{ s}^{-1}$  for 300 s), followed by a rest time of varying duration, the stress response upon the start-up of steady shear flow ( $\dot{\gamma} = 0.1\text{ s}^{-1}$ ) in the reverse direction was monitored for 300 s.

the sample was maintained quiescently (hereafter referred to as the rest time). The dependence of the stress overshoot on the rest time is a strong indication that the structure of the hybrid material evolves, even under quiescent conditions.

Possible mechanisms for the structural evolution are reorganization due to Brownian motion or strong thermodynamic interactions (i.e., aggregation). Differentiating between these two mechanisms is important, because each is consistent with a different hybrid interparticle structure. Reorganization due to Brownian motion can only be relevant if the characteristic dimension of the hybrid structure is sufficiently small. Brownian effects typically become important for structural dimensions less than 500 nm.<sup>26</sup> For the hybrid materials the critical dimension can be computed more precisely by considering the rotational diffusion of a Brownian disk. For rotational relaxation due to Brownian motion to occur on the order of  $10^4\text{ s}$  in a matrix with  $\eta_0 \sim 2000\text{ Pa}\cdot\text{s}$  at  $T = 180\text{ }^{\circ}\text{C}$ , the major axis of the disk may be no larger than 300 nm.<sup>27</sup> This analysis demonstrates that if the time scale for quiescent structural relaxation can be deduced, then the role of Brownian motion in the dynamics of the hybrids can be explored.

To further probe quiescent structural relaxation in the hybrid materials, flow reversal experiments with varying rest times were conducted for a number of hybrids having different particle loadings. The difference between the magnitude of the stress overshoot and the steady-state stress for all the conditions studied is summarized in Figure 11. This difference is a strong function of both rest time and particle loading. For example, while no stress overshoot is detectable for the 1.30 wt % hybrid, the magnitude of the stress overshoot for the 6.17 wt % does not even attain steady state by the longest rest time tested. The concentration dependence of the observed stress overshoot can be extracted by appropriate nondimensionalization. The correct scaling is reported in Figure 12. To within the error of the measurement, the effect of rest time on the nondimensional magnitude of the stress overshoot is a linear function of particle loading, since the scaling  $[(\tau_{\max}/\tau_{\infty} - 1)/c]$  generates a master curve. (The 1.30 wt % hybrid material is excluded from the analysis, since the magnitude of the stress overshoot was less than the instru-

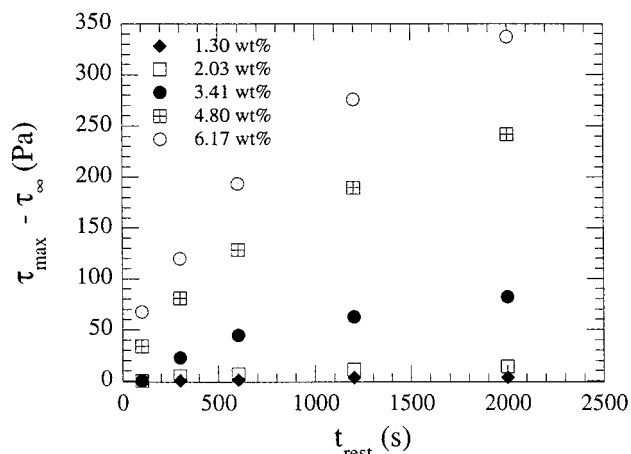


**Figure 11.** Difference between the maximum stress overshoot ( $\tau_{\max}$ ) and the steady-state stress ( $\tau_{\infty}$ ) for flow reversal experiments is plotted vs rest time for hybrid materials of various inorganic contents. Results are for  $T = 180\text{ }^{\circ}\text{C}$ .

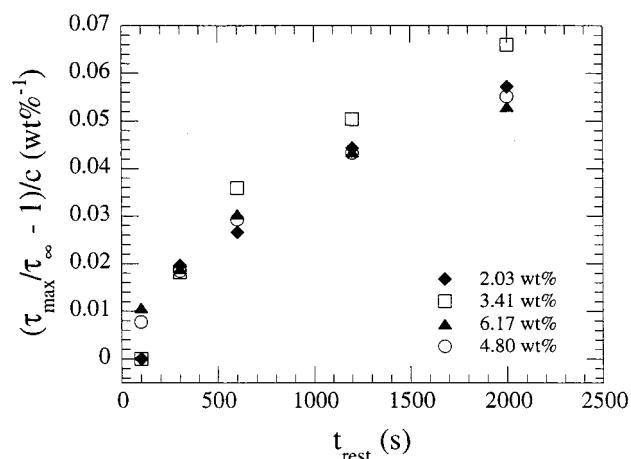


**Figure 12.** Nondimensional maximum stress overshoot of the hybrid materials scales linearly with inorganic particle loading because a plot of  $[(\tau_{\max}/\tau_{\infty} - 1)/c]$  vs  $t_{\text{rest}}$  generates a master curve.

ment resolution.) The implications of this scaling will be discussed shortly.

The stress response upon start-up of steady shear was measured at a number of shear rates to further investigate the time evolution of the stress. Results for the 4.8 wt % hybrid are plotted in Figure 13. Shear rates between 0.005 and  $1.0\text{ s}^{-1}$  were probed. Both the magnitude of the overshoot and time after the inception of flow at which it is observed are strong functions of the shear rate. The dependence can be better understood if the stress response is plotted vs strain. The resulting curves are plotted in Figure 14. The figure supports the conclusion that the stress in start-up of steady shear scales with the applied strain for this hybrid material. An analogous study was conducted for the 2.03 wt % hybrid, and the same conclusion was obtained (data not shown). Strain scaling of stress is characteristic of materials that possess no characteristic time scale. Examples of such materials include textured liquid crystalline polymer solutions and non-Brownian suspensions of rods and disks.<sup>27</sup>

Note that the stress overshoot observed in the transient rheological experiments is attributed to the inorganic particles and not the viscoelasticity of the polypropylene matrix itself. This was confirmed by observing the transient stress of pure polypropylene in start-up



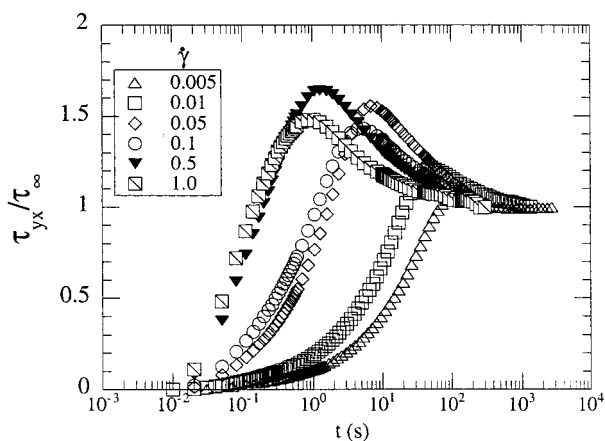


**Figure 13.** Transient shear stress measured during start-up of steady shear for the 4.8 wt % hybrid material ( $T = 180\text{ }^{\circ}\text{C}$ ; surfactant = C-18 amine; compatibilizer = PP-MA). The results of experiments at different shear rates are reported.

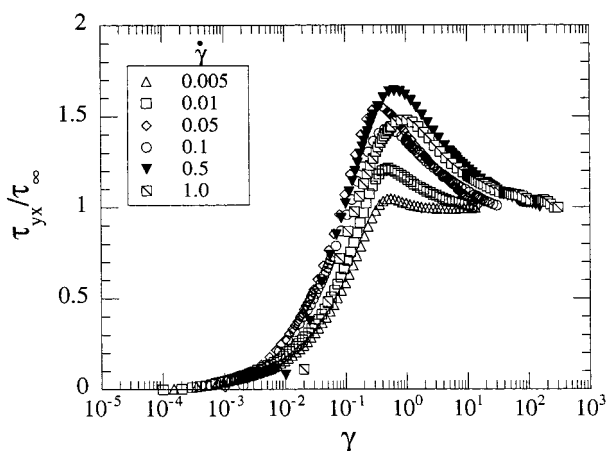


**Figure 14.** Results of Figure 13 plotted vs strain.

of steady shear. At  $180\text{ }^{\circ}\text{C}$ , the magnitude of the polypropylene overshoot was less than the instrument resolution at the highest shear rate considered in this study.

#### IV. Discussion

The linear and nonlinear rheological experiments conducted on polypropylene/montmorillonite hybrid materials have revealed a number of interesting results that can be used to understand the melt-state structure of these materials. We first summarize the key experimental findings.

For the small-amplitude oscillatory shear studies, linear rheological behavior was observed only for a limited range of strain. The storage modulus of the hybrid materials was significantly enhanced relative to the matrix polymer, particularly at low frequencies. Moreover, no terminal linear viscoelastic behavior was observed for particle loadings greater than 2.0 wt %. Finally, while not significantly affecting the WAXS-derived hybrid interlayer spacing, the choice of surfactant used to prepare the organophilic clay profoundly affected the hybrid linear viscoelastic response.

Nonlinear measurements revealed the extreme sensitivity of the rheological response to the applied deformation. The sensitivity of the stress overshoot in flow reversal experiments to the rest time implied that the structure of the hybrid materials evolved even as a

quiescent melt. In addition, the nondimensional magnitude of the stress overshoot exhibited linear scaling with concentration. The transient stress in start-up of steady shear scaled with strain over a wide range of strain rates.

In the following paragraphs, these observations are compared to previous rheological studies of nylon and polystyrene/polyisoprene nanocomposites.<sup>14–16</sup> A number of hypothetical structures of the clay hybrids are examined with respect to their ability to account for the rheological data. It is concluded that the hybrid structure most consistent with the experimental observations is one of non-Brownian, particulate domains that are thermodynamically unstable and anisometric. It is further surmised that these particulate domains consist of aggregates of multiple, ordered platelets. Finally, the relevance of the measurements to the preparation and processing of polypropylene nanocomposites is discussed.

A low-frequency plateau in the linear viscoelastic properties, such as observed in Figure 4, was found to be typical of the polypropylene hybrid materials. The absence of terminal behavior is consistent with solidlike linear viscoelastic properties, at least over the frequency range studied. This behavior could arise due to the presence of a network structure, as has been hypothesized to occur in aqueous clay suspensions.<sup>28,29</sup> Alternatively, if the characteristic dimension of the structure were small, then the mechanism for stress relaxation could be translational or rotational diffusion of the individual anisometric particles of which the structure was comprised. This hypothetical structure would produce the rheological response of a viscoelastic liquid. Yet, due to the high viscosity of the polymeric matrix, the terminal region for such Brownian relaxation would lie well below the lowest frequency probed in Figure 4. Thus, this possibility is not excluded by the data.

Deciding which of these hypothetical structures exists is of more than fundamental interest, since it is believed that the desirable end-use properties of solid-state nanocomposites are enhanced if the particles were dispersed as individual Brownian platelets. Nevertheless, linear viscoelastic measurements alone cannot determine whether the platelet structure of the hybrids is networked or dispersed. Moreover, the role of thermodynamically induced, melt-state reorganization in organoclay hybrid materials must also be considered. Particularly for the case of hydrophobic polypropylene, it is very likely that the structure obtained through melt mixing is not thermodynamically stable.<sup>20,21</sup> Like other suspensions, a thermodynamically unstable hybrid would most likely undergo gelation and network formation rather than macroscopic phase separation.<sup>26,27</sup>

The empirical observation that the onset of the stress overshoot in start-up of steady shear depends on the strain applied to the material (Figure 14), as opposed to the time after the flow has been imposed (Figure 13), can help resolve the role that Brownian motion plays in mediating the hybrid rheology. Other materials for which strain scaling of the stress has been observed are textured liquid crystalline polymers and non-Brownian suspensions of rods and disks. A common feature of these materials is that the stress response is dictated by hydrodynamics alone, since the characteristic structure or matrix viscosity is too large for Brownian relaxation to be relevant. Thus, by means of the strain scaling of the transient stress in start-up of steady



shear, it is concluded that Brownian relaxation processes do not significantly contribute to the hybrid rheological response. Alternatively, we can equivalently state that the rheological studies herein reported occur in a high Peclet number regime. Thus, the low-frequency plateau in the linear viscoelastic behavior is the result of network structure and not the orientational relaxation of individual Brownian platelets.

This conclusion is consistent with the observations herein and of Ren et al.<sup>16</sup> that the time-temperature superposition shift factors of the pure polymer and hybrid do not differ. That is, since the inorganic structure is non-Brownian, it possesses no characteristic time that scales with the thermal energy of the system, so it does not affect the polypropylene shift factors.

We next consider the characteristics of the hybrid network. Questions that arise include the following: Does the network consist of individual clay platelets, or are the platelets agglomerated into particle domains that themselves are networked? In the latter case, a hierarchy of structural length scales appears. Also, can the network be ruptured by shear deformation? If it is ruptured, will it re-form, and if so, by what mechanism? The results of flow reversal studies address these questions.

The linear concentration scaling found in the flow reversal experiments (Figure 12) demonstrates that, during nonlinear deformation, the stress response is dominated by the response of single particles or single particulate domains. (The argument stems from the fact that significant interactions between particles or particulate domains would induce nonlinear concentration effects that would not lead to the scaling observed in Figure 12.) A single particle rheological response suggests that the network is destroyed by deformation. In fact, semidilute suspensions of anisometric particles are known to exhibit a similar stress overshoot in start-up of steady shear.<sup>30</sup> The existence of the overshoot in the stress is thus linked to the distribution of particle orientations in the hybrid and the rupture of the network structure. Upon start-up of steady shear both the average orientation of the particles, and the distribution of orientations about that average orientation, evolve in response to the flow field and the hydrodynamic and potential interactions among the particles. The observation of both the stress overshoot and the linear concentration scaling indicates that the non-Brownian structure responsible for the rheological response is most likely anisometric, since rods and platelets are known to give rise to stress overshoots under non-Brownian, semidilute conditions. Moreover, according to this interpretation, the Figure 12 nondimensionalization is consistent with the particulate domain size being independent of inorganic loading, because changes in size and shape of the domains with concentration would eliminate the possibility of a linear scaling.

The non-Brownian structures that produce the stress overshoot rheology are almost certainly not individual, delaminated platelets. In light of the locally ordered platelet structure that is observed by WAXS, the structure that ruptures during the flow reversal experiments must consist of domains of multiple, ordered platelets. Thus, we conclude that a hierarchy of structures is apparent in the hybrid: locally, multiple platelets are aggregated into particulate domains that

themselves rupture, orient, and flow upon the start-up of steady shear. We note that the existence of multiplatelet structures in polystyrene/polyisoprene montmorillonite nanocomposites has also recently been deduced by consideration of X-ray diffraction and particle loading effects on the low-frequency linear viscoelastic properties.<sup>16</sup>

The origin of the quiescent structural evolution during the flow reversal experiments requires further comment. The strong shear thinning and strain sensitivity of small-amplitude oscillatory shear suggests that the hybrid network formed under quiescent conditions is easily perturbed by deformation. Upon the cessation of flow, attractive interparticle interactions would promote reconstitution of the network. Brownian motion cannot be the driving force for this reconstitution because such relaxation processes could not occur sufficiently fast to account for the changes of Figure 11. Thus, attractive interactions between the multiplatelet domains are the driving force for the structural evolution during the flow reversal experiments. The reconstituting network, which more completely re-forms as the rest time increases, is the initial state that upon deformation is oriented and ruptured, thereby giving rise to an overshoot in the stress during the flow reversal studies.

Thus, the linear and nonlinear rheological measurements are consistent with the hybrid structure of a weakly agglomerated network of multiplatelet particulate domains that is ruptured and reconstituted under flow and quiescent conditions, respectively. The mesoscopic particulate domains of multiple, ordered platelets, which are the dominant structure for nonlinear deformation, are non-Brownian and anisometric. Attractive interactions among the multiplatelet domains give rise to quiescent structural evolution and network re-formation after cessation of shear.

Finally, we remark upon the surprising sensitivity of the linear viscoelastic measurements to surfactant chemistry. While the storage modulus was a strong function of chemistry, the WAXS-derived interlayer spacing was nearly unaffected by the changes. This comparison is useful: First, it shows that the local ordering of the clay layers is nearly insensitive to chemistry, perhaps because the extreme hydrophobicity of the polypropylene matrix renders substantial intercalation and exfoliation too unfavorable.<sup>21</sup> Second, it indicates that the configuration and interactions of the mesoscopic multiplatelet domain structure must be strongly affected by the choice of surfactant because of the large changes plotted in Figure 8.

Reasons for why the choice of surfactant affects the rheology but not the local clay ordering is the subject of current study. It is possible that differences in the surfactant adsorbed to the exterior surface of the multiplatelet domains mediates differences in the attractive interparticle interactions that give rise to the hybrid network. Alternatively, the size and shape of the multiplatelet domains could depend on surfactant chemistry. Such subtle changes in the mesoscopic structure would be poorly characterized by WAXS yet could yield large rheological effects. Whatever the origin of the effect, Figure 8 suggests that the surfactant does indeed play a role in determining whether the hybrid structure is networked, since the low-frequency plateau characteristic of network structure is absent for some of the surfactant combinations. Dynamic mechanical analysis demonstrates that these differences in linear viscoelas-

ticity can be related to trends in the solid-state tensile modulus of the hybrids.<sup>31</sup>

In conclusion, rheological methods probe hybrid structure only indirectly; however, the distinctive features of nonlinear measurements and the sensitivity of linear viscoelasticity to surfactant chemistry reported here demonstrate that such methods can provide a useful characterization of nanocomposite structure, particularly at the mesoscopic level. Thus, this work demonstrates the scope for using rheology (and other techniques that characterize nanoscopic length scales such as small-angle X-ray scattering) in conjunction with standard methods such as WAXS, electron microscopy, and mechanical testing to provide a more complete characterization of the structure and properties of new nanocomposite materials.

**Acknowledgment.** We are grateful to Professors John Halloran and Albert Yee for use of blending equipment and dynamic mechanical analysis instrumentation, respectively. Equistar Chemicals, Uniroyal Chemical, BASF, and Southern Clay Products kindly provided materials used in this study. We also acknowledge the assistance of Dr. Laraba Kendig and Catherine Eehalt during the study. This research was supported in part by Honda Research and Development, Ltd. A.S.A and A.S. acknowledge fellowships provided by Kuwait University and the Royal Thai government, respectively.

## References and Notes

- (1) Kojima, Y.; Usuki, A.; Kawasumi, M.; Okada, A.; Fukushima, Y.; Kurauchi, T.; Kamigaito, O. *J. Mater. Res.* **1993**, *8*, 1185.
- (2) Lan, T.; Pinnavaia, T. J. *Chem. Mater.* **1994**, *6*, 2216.
- (3) Messersmith, P. B.; Giannelis, E. P. *J. Polym. Sci., Part A: Polym. Chem.* **1995**, *33*, 1047.
- (4) Gilman, J. W.; Kashiwagi, T.; Lichtenhan, J. D. *SAMPE J.* **1997**, *33*, 40.
- (5) Dagani, R. *Chem. Eng. News* **1999**, *77*, 25.
- (6) Shi, H.; Lan, T.; Pinnavaia, T. J. *Chem. Mater.* **1996**, *8*, 1584.
- (7) Usuki, A.; Kojima, Y.; Kawasumi, M.; Okada, A.; Fukushima, Y.; Kurauchi, T.; Kamigaito, O. *J. Mater. Res.* **1993**, *8*, 1179.
- (8) Vaia, R. A.; Ishii, H.; Giannelis, E. P. *Chem. Mater.* **1993**, *5*, 1694.
- (9) Cho, J. W.; Paul, D. R., submitted for publication.
- (10) Reichert, P.; Nitz, H.; Klinke, S.; Brandsch, R.; Thomann, R.; Mülhaupt, R. *Macromol. Mater. Eng.* **2000**, *375*, 8.
- (11) Kawasumi, M.; Hasegawa, N.; Kato, M.; Usuki, A.; Okada, A. *Macromolecules* **1997**, *30*, 6333.
- (12) Vaia, R. A.; Jandt, K. D.; Kramer, E. J.; Giannelis, E. P. *Macromolecules* **1995**, *28*, 8080.
- (13) Vaia, R. A.; Sauer, B. B.; Tse, O. K.; Giannelis, E. P. *J. Polym. Sci., Part B: Polym. Phys.* **1997**, *35*, 59.
- (14) Krishnamoorti, R.; Vaia, R. A.; Giannelis, E. P. *Chem. Mater.* **1996**, *8*, 1728.
- (15) Krishnamoorti, R.; Giannelis, E. P. *Macromolecules* **1997**, *30*, 4097.
- (16) Ren, J.; Silva, A. S.; Krishnamoorti, R. *Macromolecules* **2000**, *33*, 3739.
- (17) Kurokawa, Y.; Yasuda, H.; Kashiwagi, M.; Oyo, A. *J. Mater. Sci., Lett.* **1997**, *16*, 1670.
- (18) Hasegawa, N.; Kawasumi, M.; Kato, M.; Usuki, A.; Okada, A. *J. Appl. Polym. Sci.* **1998**, *67*, 87.
- (19) Kato, M.; Usuki, A.; Okada, A. *J. Appl. Polym. Sci.* **1997**, *66*, 1781.
- (20) Ginzburg, V. V.; Balazs, A. C. *Macromolecules* **1999**, *32*, 5681.
- (21) Balazs, A. C.; Singh, C.; Zhulina, E. *Macromolecules* **1998**, *31*, 8370.
- (22) Sclavons, M.; Franquient, P.; Carlier, V.; Verfaillie, G.; Fallais, I.; Legras, R.; Laurent, M.; Thyron, F. C. *Polymer* **2000**, *41*, 1989.
- (23) Li, S.; Jarvela, P. K.; Jarvela, P. A. *J. Appl. Polym. Sci.* **1999**, *71*, 1649.
- (24) Ho, R. M.; Su, A. C.; Wu, C. H.; Chen, S. I. *Polymer* **1993**, *34*, 3264.
- (25) Walker, L. M.; Wagner, N. J.; Larson, R. G.; Mirau, P. A.; Moldenaers, P. *J. Rheol.* **1995**, *39*, 925.
- (26) Russel, W. B.; Saville, D. A.; Schowalter, W. R. *Colloidal Dispersions*; Cambridge University Press: Cambridge, 1989.
- (27) Larson, R. G. *The Structure and Rheology of Complex Fluids*; Oxford University Press: New York, 1999.
- (28) van Olphen, H. *An Introduction of Clay Colloid Chemistry*; J. Wiley & Sons: New York, 1977.
- (29) Jogun, S.; Zukoski, C. F. *J. Rheol.* **1996**, *40*, 1211.
- (30) Powell, R. L. *J. Stat. Phys.* **1991**, *62*, 1073.
- (31) Somwangthanaroj, A.; Solomon, M. J., manuscript in preparation.

MA001122E